

Bacterial biofilm shows persistent resistance to liquid wetting and gas penetration

Alexander K. Epstein^a, Boaz Pokroy^{a,1}, Agnese Seminara^b, and Joanna Aizenberg^{a,c,d,2}

^aSchool of Engineering and Applied Sciences, Harvard University, 29 Oxford Street, Cambridge, MA 02138; ^bKavli Institute for Bionano Science and Technology and School of Engineering and Applied Sciences, Harvard University, Cambridge, MA 02138; ^cDepartment of Chemistry and Chemical Biology, Harvard University, 12 Oxford Street, Cambridge, MA 02138; and ^dWyss Institute for Biologically Inspired Engineering, 3 Blackfan Circle, Boston, MA 02115

Edited by Jerry P. Gollub, Haverford College, Haverford, PA, and approved November 19, 2010 (received for review July 29, 2010)

Most of the world's bacteria exist in robust, sessile communities known as biofilms, ubiquitously adherent to environmental surfaces from ocean floors to human teeth and notoriously resistant to antimicrobial agents. We report the surprising observation that *Bacillus subtilis* biofilm colonies and pellicles are extremely nonwetting, greatly surpassing the repellency of Teflon toward water and lower surface tension liquids. The biofilm surface remains nonwetting against up to 80% ethanol as well as other organic solvents and commercial biocides across a large and clinically important concentration range. We show that this property limits the penetration of antimicrobial liquids into the biofilm, severely compromising their efficacy. To highlight the mechanisms of this phenomenon, we performed experiments with mutant biofilms lacking ECM components and with functionalized polymeric replicas of biofilm microstructure. We show that the nonwetting properties are a synergistic result of ECM composition, multiscale roughness, reentrant topography, and possibly yet other factors related to the dynamic nature of the biofilm surface. Finally, we report the impenetrability of the biofilm surface by gases, implying defense capability against vapor-phase antimicrobials as well. These remarkable properties of *B. subtilis* biofilm, which may have evolved as a protection mechanism against native environmental threats, provide a new direction in both antimicrobial research and bioinspired liquid-repellent surface paradigms.

antimicrobial resistance | microcomputed tomography | biofilm hydrophobicity | liquid repellency | nonwettability

Contrary to what was believed as recently as 20 years ago, bacteria exist in nature predominantly as members of biofilms—structured, multicellular communities adherent to surfaces in natural and man-made environments (1). Biofilm formation is now known to cause contamination of plumbing, oil wells, medical implants, building heating, ventilation, air conditioning and other systems (2) and is largely responsible for nearly 100,000 nosocomial deaths annually in the United States and 80% or more of all microbial infections in humans (3, 4). Antimicrobial products have become extensively used to combat biofilm contamination in health care, agriculture, and industrial settings, and increasingly by the general public as well (5). Commercial products employ a wide variety of active chemical agents, or biocides, often delivered in liquid form and sometimes as vapor. Indeed, one review of antiseptics and disinfectants identifies 12 classes of liquid agents and 5 common types of vapor-phase sterilants (5). Most of these biocides act on multiple intracellular targets. For example, chlorhexidine congeals the cytoplasm and disrupts the inner membrane, formaldehyde cross-links macromolecules such as DNA, and peroxygens oxidize the thiol groups in enzymes and proteins. Other liquids, such as ethanol, among the most universal of antiseptics and disinfectants, need only access the cell membrane, as the mode of action is believed to be membrane damage and protein denaturation. Common vapor-phase biocides include ethylene oxide and formaldehyde, both

broad-spectrum alkylating agents that attack proteins and other organic compounds (5).

Regardless of the particular chemistry or mechanism, the biocide must be able to reach the target cell to cause damage. At the multicellular level, therefore, the effective biocide must penetrate into the ECM—the slime-like “cement” of biofilm. Biofilms, however, offer their member cells several benefits, in particular, protection from environmental threats. It has been reported that ECM acts as a diffusion barrier and as a charged binding filter for certain antibiotics (6), and that it complements enzymes and multidrug resistance pumps on cells that remove antimicrobials (7, 8). The ECM composition varies widely among species, but in general its major components are exopolysaccharides and proteins (9). The resistance to threats covers a wide range of treatments: Biofilms exposed to chlorine bleach for 60 min are reported to still have live cells (3); biofilms in pipes continuously flushed over 7 d with multiple biocides recolonize the pipes (10), and biofilms have been reported to survive in bottled iodine solution for up to 15 mo (11). Yet the remarkable robustness of biofilms against a broad range of antimicrobials, which differ entirely in chemistry and mechanism, remains a puzzle, despite two decades of biofilm research.

We report herein a striking phenomenon that we believe may be a critical property responsible for biofilm integrity and biocide resistance. The surfaces of *Bacillus subtilis* biofilms are strongly liquid repellent—nonwetting—against a broad range of solvents and commercial biocides. Similar to water that is repelled by the lotus leaf (12), these liquids do not spread on and into the biofilm surface. However, although the lotus leaf is merely hydrophobic, i.e., it repels water but is quickly wetted by liquids of lower surface tension*, *B. subtilis* biofilms resist even ethanol concentrations on the order of 80%. Additionally, we report that the biofilm can effectively resist penetration by applied vapors, even following prolonged exposure. These results reveal the need to understand the bulk-phase, macroscopic aspects of biocide interaction with the biofilm surface in addition to the molecular interactions with the matrix interior and cells, where biocides ultimately act. Critical limitations may not be recognized if the resistance is not first addressed at the level of liquid wettability and effective biocide access to the biofilm interior.

Author contributions: A.K.E., B.P., and J.A. designed research; A.K.E., B.P., and A.S. performed research; A.K.E., B.P., A.S., and J.A. analyzed data; and A.K.E. and J.A. wrote the paper.

The authors declare no conflict of interest.

This article is a PNAS Direct Submission.

Freely available online through the PNAS open access option.

*We refer to the surface tension of a liquid–air interface as the “surface tension of the liquid.”

¹Present address: Department of Materials Engineering and the Russell Berrie Nanotechnology Institute, Technion—Israel Institute of Technology, Haifa 32000, Israel.

²To whom correspondence should be addressed. E-mail: jaiz@seas.harvard.edu.

This article contains supporting information online at www.pnas.org/lookup/suppl/doi:10.1073/pnas.1011033108/-DCSupplemental.

Table 2. Commercial biocides on *B. subtilis* WT biofilms

Test liquid	Contact angle (°)
Clorox bleach	45.9 ± 9.4
Lysol Professional	121.9 ± 6.3
Hibiclens	130.8 ± 10.2
Drain opener (10 s)	123.0 ± 13.7
Drain opener (5 min)	47.0 ± 0.52

Error = standard deviation; $n = 9$

To identify the underlying biochemical and physical features of the biofilm that might be responsible for this behavior, we performed a similar analysis for *B. subtilis* mutants that lack or overexpress primary ECM components. Along with the wild-type biofilm, we prepared three mutants: exopolysaccharide-deficient (epsH), matrix protein-deficient (tasA), and overproduced exopolysaccharide and protein (sinR) (14). Each of the phenotypes is shown in Fig. 4. The epsH biofilms are completely wetted by ethanol at any concentration, and even by pure water. Consequently, exposure of the epsH mutant to a rhodamine-labeled liquid results in a uniform fluorescent signal, confirming complete penetration of the rhodamine solution into the biofilm (Fig. 2B and Movie S2). Although the epsH biofilms are also wetted by 50% solutions of other low-surface-tension liquids, such as methanol, isopropanol, or acetone, the tasA biofilms show moderate repellency, with a contact angle of ~110–120° for these liquids (Table 1). Hence, the exopolysaccharide plays a primary critical role in biofilm repellency, whereas the tasA protein appears to play a secondary, indirect role, although the fact that neither the matrix protein nor the polysaccharides individually preserve biofilm repellency shows that both of these biomolecules are required for full resistance. In contrast to the epsH and tasA mutants, sinR biofilms with overexpressed polysaccharide and protein components show persistent liquid repellency, only slightly inferior to that of the wild type (see Fig. 4). The corresponding wild-type and matrix-mutant pellicles exhibit the same qualitative wetting behaviors as colonies.

We note that in addition to the chemical contribution of surface molecules, the wetting properties of materials are known to be modified by complex surface microstructure (15, 16). In particular, wild-type biofilm's micro- and nanoscale features with highly reentrant curvatures (Fig. 5A) may be as important for this wetting resistance at lower surface tensions (17). Indeed, the epsH and tasA mutants lack the wrinkled architecture of the wild

type, whereas the sinR mutant slightly overexpresses the larger scale wrinkled topography (14) but appears smoother than the wild type at the 10- to 100- μm scale (Fig. 4B and Fig. S2). To clarify the potential role of the biofilm microstructure, we replicated the biofilm in epoxy resin (18) and verified by scanning electron microscopy (SEM) that the topography of the polymeric replicas reproduced the complex features of the biofilm at the micron level (Fig. 5B) (19). Creating a geometric replica allows the topography and surface chemistry to be decoupled, as the surface chemistry can then be separately modified. We fabricated a series of epoxy biofilm replicas as well as flat epoxy surfaces, each with and without hydrophobic coating, and compared the contact angle as a function of ethanol concentration (Fig. 5C). For a pure water droplet, the microtopography of the unmodified wild-type replicas alone renders the surfaces moderately hydrophobic, with a contact angle of ~115°, whereas the same flat surface is mildly hydrophilic (contact angle ~85°). Moreover, fluorinated wild-type replicas, which combine native microtopography with hydrophobic surface chemistry, reproduce the ~135° hydrophobicity level of the native biofilm. Droplets containing ethanol, however, do not follow this behavior: None of the replicas reproduce the nonwetting plateau typical of the live biofilm. In particular, all of the replicas—including those with both the wild-type topography and hydrophobic coating—undergo a pseudolinear drop in contact angle with increasing ethanol concentration (Fig. 5C), similar to Teflon (Fig. 1). These results suggest that both the topographic and surface chemistry features of the extracellular matrix work together to give the biofilm its highly nonwetting behavior toward water, but that topography and simple hydrophobic chemistry cannot completely account for the observed extreme repellency of the biofilm surface toward low-surface-tension liquids.

In addition to liquids, many environmental threats to bacterial biofilms, and indeed, quite a number of antimicrobials reported over the last five decades (20–23), are presented to the surface in vapor phase. Therefore we also investigated surface gas penetration of wild type as well as matrix-altered *B. subtilis* biofilms. To assess how readily a gas penetrates into the biofilm, we prepared the biofilm (as described in *Materials and Methods*) and exposed it to a test vapor that deposited a radiation contrast agent wherever it could access on or in the sample, therefore revealing the extent of penetration upon X-ray imaging (vapor was presented by atomic layer deposition as described in *Materials and Methods*).

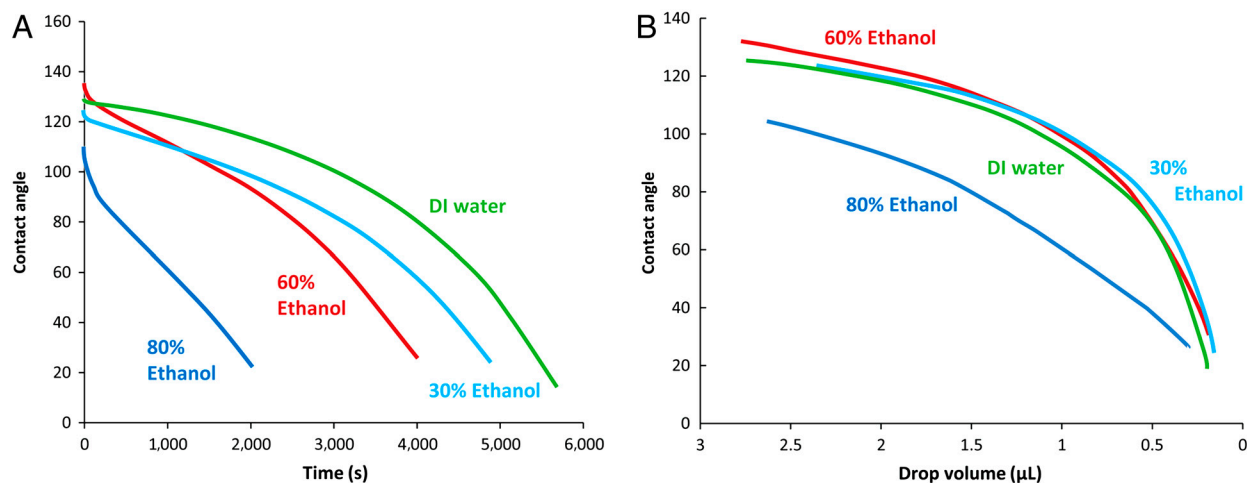


Fig. 3. Persistent biofilm nonwettability is invariable with respect to ethanol concentration across the repellent concentration range. Drops of four ethanol-water concentrations were tracked for contact angle during evaporation on the surfaces of wild-type *B. subtilis* colonies. (A) Evaporation contact angles decay faster in time for higher ethanol concentrations. This is expected due to ethanol's high vapor pressure and due to some contact line pinning, or sticking of the droplet edge to surface heterogeneities (16). (B) The evaporation contact angle as a function of drop volume, however, traces the same curve for deionized water, 30%, and 60% ethanol, in spite of dramatic surface tension decrease, and shows large deviation only at the 80% grade—roughly the threshold concentration between nonwetting and wetting behavior.

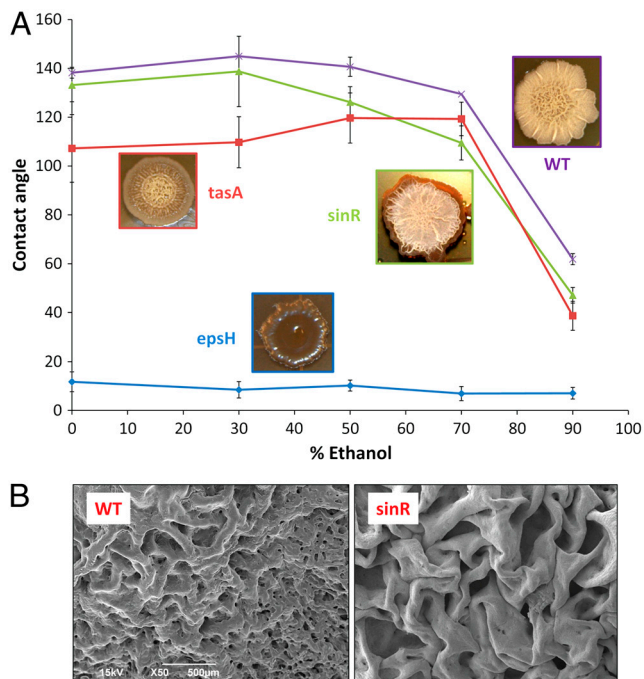


Fig. 4. Characterization of liquid repellency mechanisms using genetic mutants of *B. subtilis* biofilms lacking either the carbohydrate-rich epsH or protein tasA, or sinR. (A) The phenotypes are inset adjacent to their respective contact angle curves. Highly wrinkled sinR biofilm, with excess tasA protein and epsH, exhibits slightly decreased repellency relative to wild type, possibly related to suboptimal topography. Error bars are SD, $n = 7$ for WT and Teflon, $n = 8+$ for tasA, $8+$ for epsH, and $12+$ for sinR. A standard Wilcoxon two-sided test was performed to test statistical significance in contact angle differences (1% and 5% significance level). The contact angle for epsH is statistically different from any other strain; WT is statistically different from tasA at all ethanol concentrations, and from sinR at ethanol concentrations $\geq 50\%$; tasA and sinR are statistically different except at 50% and 90% ethanol concentration (and 70% at significance level 1%). (B) Corresponding magnification SEM images showing the surface features of the critical point dried WT biofilm (Left) and the sinR mutant (Right).

We imaged the biofilm using synchrotron-generated X-rays and microcomputed tomography (see *Materials and Methods*). Regions of high intensity within the biofilm indicate where the gas has penetrated and alumina has been deposited. In all the wild-type samples, the images show a sharp gradient of intensity close to the surface as shown in Fig. 6A: The gas penetrates only about $10\ \mu\text{m}$ below the surface. However, penetration is markedly deeper in the tasA and epsH mutants, as shown by the much thicker bright region in Fig. 6B and C. Thus, as for liquid repellency, biofilm gas impenetrability also requires both the protein and the polysaccharide matrix components.

Discussion

The presented data uncovers a previously undescribed phenomenon: *Bacillus subtilis* biofilm colonies and pellicles are extremely liquid and gas repellent, greatly surpassing the properties of known repellent surfaces such as Teflon and Lotus leaves. We demonstrate that the biofilm surface is persistently nonwetting against up to 80% ethanol as well as other organic solvents and commercial biocides. We show that the biofilm nonwetting properties arise from both the polysaccharide and protein components of the extracellular matrix and are a synergistic result of surface chemistry, multiscale surface roughness, and reentrant topography. Moreover, we report the gas impenetrability of the biofilm surface, implying defense capability against vapor-phase antimicrobials as well.

Biofilms underlie a growing public threat in the form of nosocomial deaths, contaminated water, sick-building syndrome

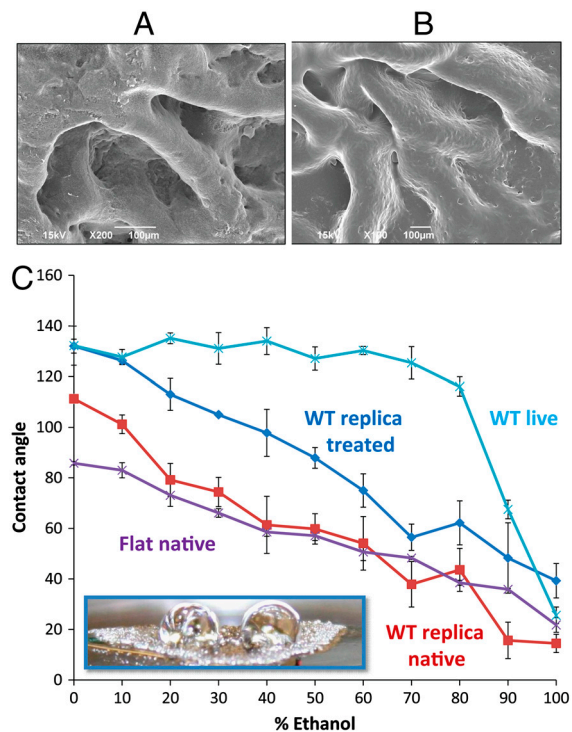


Fig. 5. Testing role of topography using functionalized polymeric replicas of biofilm microstructure. (A) SEM image showing the surface features of the critical point dried live WT biofilm; (B) SEM image showing the surface features of the UV-cured epoxy replica of the wild-type biofilm. Microscale topography is reproduced well, although dehydration artifacts may occur in the critical point dried sample. (C) Contact angle of a live wild-type colony, a native (uncoated) epoxy replica fabricated by adapting soft lithography (18), a fluorinated replica, and a native (uncoated) flat epoxy substrate. (Inset) Epoxy biofilm replica with applied drops of 30% ethanol. Error bars are SD, $n = 7$.

(occupant illness due to airborne contaminants), etc. To our knowledge the effort to control them has not considered the possibility that biocides might be resisted simply on account of being liquids or gases. Although antiseptics and disinfectants have become ubiquitous, they are clearly not optimized for biofilms. Persistent biofilm nonwettability and gas impenetrability therefore represent significant obstacles against many of our most commonly used biocides: Because liquids and gases cannot fully penetrate into the matrix, they cannot access all the subsurface cells and are largely ineffective. Our results reveal the need to study biocide resistance in terms of the macroscopic interaction with the biofilm surface in addition to the molecular-scale interactions with the matrix molecules and cells. Such insight could help address the long-standing question of how a broad range of antimicrobials that differ entirely in chemistry and mechanism can all fail. Our findings further suggest that future delivery strategies may be severely compromised if they do not take into account the level of liquid wettability or gas penetration—to be effective against biofilms, antimicrobial delivery may well require a solvent or diluent specifically designed to penetrate into the biofilm surface. If surface properties are highly species-specific, approaching antimicrobial design from this perspective could also provide a way to selectively target particular biofilms.

B. subtilis biofilms grow in exposure to air, potentially extending our findings to biofilm communities in a wide range of environments, such as air ducts, sewers, liquid storage tanks, and porous soil media. These liquid repellency properties may in fact have evolved in response to *B. subtilis*'s natural environment, soil, where water leaches heavy metals, antibiotics, and other toxins. Interestingly, *B. subtilis* is now being used for crop protection

and placed in a small Petri dish. The PDMS mold thermally cured at room temperature for 24 h. After curing, the agar was easily removed from the PDMS and the remaining biofilm "master" was fully dissolved during 15 min of sonication in a bath using a mixture of 1 part chlorine bleach, 1 part acetic acid, and 4 parts deionized water. The negative PDMS mold was also cleaned with ethanol, isopropanol, and acetone. To produce polymer replicas of the colony, the commercial UV-initiated one-part epoxy UVO-114 (Epoxy Technology) was chosen. Multiple epoxy replicas of the 1-wk-old WT colony were fabricated; also, multiple flat UVO-114 epoxy replicas of a glass slide were fabricated by the PDMS molding method. Half of the colony and glass slide replicas were left as native epoxy surfaces, whereas half were sputter-coated with 10 nm Pt/Pd and hydrophobized by perfluorodecane-thiol in vapor-phase deposition.

Imaging. Critical point drying of biofilm colonies for SEM comparison to replicas was performed as follows: Samples of wild type, *tasA* mutant, and *epsH* mutant *B. subtilis* colonies were fixed in glutaraldehyde for 1 h at multiples of 12 h after drop-casting 3 μ L of LB culture onto MSgg agar plates. After fixing, the samples were stepped through 10% grades of ethanol, given at least 30 min per step, and allowed to completely dehydrate overnight in absolute ethanol. They were then critical point dried on a Tousimis Auto Samdri 815 Series A. Imaging to compare the dried and epoxy replicated biofilm was performed on a Zeiss field emission Ultra55 SEM. To assay penetration of liquid into colony texture, rhodamine diluted 1:500 in deionized (DI) water was placed dropwise on a *B. subtilis* WT and *epsH* colony until it formed a puddle; after waiting 1 min, it was blown off by compressed air. Fluorescent microscopy *z* stacks in a 6 \times 6 tile pattern, covering a 1.2 \times 1.2 mm total field of view and the depth range of fluorescent signal, were taken on a Leica TCS SP5 scanning laser confocal. The *z* stacks were merged in Leica software and a maximum intensity merge was obtained with ImageJ.

Microcomputed Tomography. Critical point dried samples of wild-type, *tasA* mutant, and *epsH* mutant *B. subtilis* colonies were coated for 1 h in a Cambridge NanoTech Savanah 200 Atomic Layer Deposition chamber sequentially with trimethylaluminum precursor gas that deposits alumina (Al₂O₃) at 45 °C and hafnia (HfO₂) at 65 °C. This was done in order to assess penetration of the precursor gases while simultaneously providing X-ray radiation contrast. On site at the Argonne National Lab, Advanced Photon Source, Station 13-BMD, the samples were carefully sectioned by razor and each mounted into a 2-mm inner diameter hollow plastic tube. Each sample was mounted in a three-jaw chuck and imaged over a 360° rotation, with a beam energy of 40 kV. Radiographs of ~3 μ m/pixel resolution were reconstructed into 3D volumes using the IDL software package and analyzed. Parts of the biofilm that were less dense and more porous were more permeable to gas diffusion and hence to oxide deposition. Areas that had heavier oxide deposition absorbed more radiation, producing darker transmission images.

ACKNOWLEDGMENTS. We are grateful to Dr. Moshe Shemesh, Dr. Yunrong (Win) Chai, and Dr. Ilana Kolodkin-Gal (Department of Molecular and Cellular Biology, Harvard University, Cambridge, MA) for providing plates and cultures as well as guidance in biological technique, to Dr. Hera Vlamakis and Dr. Allon Hochbaum for advice on biological protocols, and to Dr. Thomas Angelini for assistance with confocal microscopy. We thank Prof. Richard Losick for use of his laboratory facilities, Dr. Alison Grinthal for assistance with the manuscript, and Dr. Mark Rivers for training and help at Beamline 13-BMD at the Advanced Photon Source. This work was funded by the BASF Advanced Research Initiative at Harvard University. Use of the Advanced Photon Source was supported by the US Department of Energy, Office of Science, Office of Basic Energy Sciences, under Contract W-31-109-Eng-38.

- Aguilar C, Vlamakis H, Losick R, Kolter R (2007) Thinking about *Bacillus subtilis* as a multicellular organism. *Curr Opin Microbiol* 10:638–643.
- Costerton JW, Stewart PS (2001) Battling biofilms—The war is against bacterial colonies that cause some of the most tenacious infections known. The weapon is knowledge of the enemy's communication system. *Sci Am* 285(1):74–81.
- Davies D (2003) Understanding biofilm resistance to antibacterial agents. *Nat Rev Drug Discov* 2:114–122.
- Klevens RM, et al. (2007) Estimating health care-associated infections and deaths in US hospitals, 2002. *Public Health Rep* 122:160–166.
- McDonnell G, Russell AD (1999) Antiseptics and disinfectants: Activity, action, and resistance. *Clin Microbiol Rev* 12:147–179.
- Ishida H, et al. (1998) In vitro and in vivo activities of levofloxacin against biofilm-producing *Pseudomonas aeruginosa*. *Antimicrob Agents Chemother* 42:1641–1645.
- Giwerzman B, Jensen ET, Hoiby N, Kharazmi A, Costerton JW (1991) Induction of beta-lactamase production in *Pseudomonas aeruginosa* biofilm. *Antimicrob Agents Chemother* 35:1008–1010.
- Lomovskaya O, Lewis K (1992) Emr, an *Escherichia coli* locus for multidrug resistance. *Proc Natl Acad Sci USA* 89:8938–8942.
- Branda SS, Vik A, Friedman L, Kolter R (2005) Biofilms: The matrix revisited. *Trends Microbiol* 13:20–26.
- Anderson RL, Holland BW, Carr JK, Bond WW, Favero MS (1990) Effect of disinfectants on pseudomonads colonized on the interior surface of PVC pipes. *Am J Public Health* 80:17–21.
- Panlilio AL, et al. (1992) Infections and pseudoinfections due to povidone-iodine solution contaminated with *Pseudomonas cepacia*. *Clin Infect Dis* 14:1078–1083.
- Barthlott W, Neinhuis C (1997) Purity of the sacred lotus, or escape from contamination in biological surfaces. *Planta* 202:1–8.
- Branda SS, Gonzalez-Pastor JE, Ben-Yehuda S, Losick R, Kolter R (2001) Fruiting body formation by *Bacillus subtilis*. *Proc Natl Acad Sci USA* 98:11621–11626.
- Branda SS, Chu F, Kearns DB, Losick R, Kolter R (2006) A major protein component of the *Bacillus subtilis* biofilm matrix. *Mol Microbiol* 59:1229–1238.
- Cassie ABD, Baxter S (1944) Wettability of porous surfaces. *T Faraday Soc* 40:546–550.
- Roach P, Shirtcliffe NJ, Newton MI (2008) Progress in superhydrophobic surface development. *Soft Matter* 4:224–240.
- Tuteja A, et al. (2007) Designing superoleophobic surfaces. *Science* 318:1618–1622.
- Pokroy B, Epstein AK, Persson-Gulda MCM, Aizenberg J (2009) Fabrication of bioinspired actuated nanostructures with arbitrary geometry and stiffness. *Adv Mater* 21:463–469.
- Furstner R, Barthlott W, Neinhuis C, Walzel P (2005) Wetting and self-cleaning properties of artificial superhydrophobic surfaces. *Langmuir* 21:956–961.
- Dorman HJD, Deans SG (2000) Antimicrobial agents from plants: Antibacterial activity of plant volatile oils. *J Appl Microbiol* 88:308–316.
- Hoffman RK, Warshowsky B (1958) Beta-propiolactone vapor as a disinfectant. *Appl Microbiol* 6:358–362.
- Sapers GM, Walker PN, Sites JE, Annous BA, Eblen DR (2003) Vapor-phase decontamination of apples inoculated with *Escherichia coli*. *J Food Sci* 68:1003–1007.
- Simmons GF, Smilanick JL, John S, Margosan DA (1997) Reduction of microbial populations on prunes by vapor-phase hydrogen peroxide. *J Food Protect* 60:188–191.
- Bais HP, Fall R, Vivanco JM (2004) Biocontrol of *Bacillus subtilis* against infection of Arabidopsis roots by *Pseudomonas syringae* is facilitated by biofilm formation and surfactin production. *Plant Physiol* 134:307–319.
- Angelini TE, Roper M, Kolter R, Weitz DA, Brenner MP (2009) *Bacillus subtilis* spreads by surfing on waves of surfactant. *Proc Natl Acad Sci USA* 106:18109–18113.
- Be'er A, et al. (2009) *Paenibacillus dendritiformis* bacterial colony growth depends on surfactant but not on bacterial motion. *J Bacteriol* 191:5758–5764.
- Gao XF, Jiang L (2004) Water-repellent legs of water striders. *Nature* 432:36.
- Blossey R (2003) Self-cleaning surfaces—Virtual realities. *Nat Mater* 2:301–306.
- Aussillous P, Quere D (2001) Liquid marbles. *Nature* 411:924–927.
- Feng L, et al. (2002) Super-hydrophobic surfaces: From natural to artificial. *Adv Mater* 14:1857–1860.
- Tuteja A, Choi W, Mabry JM, McKinley GH, Cohen RE (2008) Robust omniphobic surfaces. *Proc Natl Acad Sci USA* 105:18200–18205.
- Ahuja A, et al. (2008) Nanonails: A simple geometrical approach to electrically tunable superlyophobic surfaces. *Langmuir* 24:9–14.